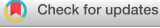


RESEARCH PAPER

 OPEN ACCESS 

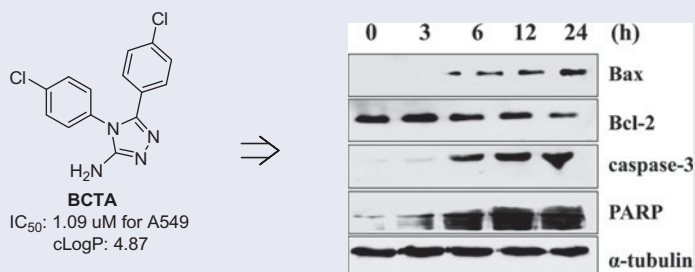
Synthesis, activity evaluation, and pro-apoptotic properties of novel 1,2,4-triazol-3-amine derivatives as potent anti-lung cancer agents

Xian-yu Sun^a, Chun-yan Zhong^a, Qing-qing Qiu^a, Zhen-wang Li^a, Mei-yu Liu^a, Xin Wang^a and Cheng-hao Jin^b 

^aDepartment of Pharmacy, College of Animal Science and Technique, Heilongjiang Bayi Agricultural University, Daqing, China; ^bDepartment of Biochemistry and Molecular Biology, College of Life Science and Technology, Heilongjiang Bayi Agricultural University, Daqing, China

ABSTRACT

In this study, a series of 4,5-bis(substituted phenyl)-4H-1,2,4-triazol-3-amine compounds was designed, synthesised, and evaluated to determine their potential as anti-lung cancer agents. According to the results of screening of lung cancer cell lines A549, NCI-H460, and NCI-H23 *in vitro*, most of the synthesised compounds have potent cytotoxic activities with IC₅₀ values ranging from 1.02 to 48.01 μM. Particularly, compound 4,5-bis(4-chlorophenyl)-4H-1,2,4-triazol-3-amine (**BCTA**) was the most potent anti-cancer agent, with IC₅₀ values of 1.09, 2.01, and 3.28 μM against A549, NCI-H460, and NCI-H23 cells, respectively, meaning many-fold stronger anti-lung cancer activity than that of the chemotherapeutic agent 5-fluorouracil. We also explored the effects of **BCTA** on apoptosis in lung cancer cells by flow cytometry and western blotting. Our results indicated that **BCTA** induced apoptosis by upregulating proteins BAX, caspase 3, and PARP. Thus, the potential application of compound **BCTA** as a drug should be further examined.



An outstanding compound **BCTA** (4,5-bis(4-chlorophenyl)-4H-1,2,4-triazol-3-amine) was found to possess more potent anticancer activity against several lung cancer cells than the reference drugs 5-FU. The effects of **BCTA** on apoptosis and necrosis in A549 cells were analysed by Hoechst/propidium iodide (PI) double staining and early and late apoptosis were analysed by Annexin V/PI flow cytometry. Further Western blotting results revealed that **BCTA** could induce cell apoptosis by down-regulating Bcl-2 protein.

ARTICLE HISTORY

Received 3 April 2019
Revised 23 May 2019
Accepted 19 June 2019

KEYWORDS

Synthesis; anti-cancer; lung cancer; apoptosis; BCL-2

1. Introduction

According to one study, lung cancer ranks first in cancer mortality worldwide, and the number of cases is currently increasing. In 2018, nearly 1,972,000 new lung cancer cases and 1,748,000 lung cancer deaths occurred globally¹. Therefore, the discovery and/or synthesis of novel anti-cancer agents is necessary for eliminating this urgent global health problem. The discovery of novel anti-cancer agents with highly effective modes of action against tumours is an important and challenging task.

Triazole and its derivatives have a broad range of biological and pharmacological properties, such as anti-bacterial, anti-human immunodeficiency virus², anti-microbial³, anti-fungal⁴, anti-viral⁵, and anti-cancer effects^{6–14}. For example, Abdou *et al.* designed and synthesised the triazole structure of amino-thiadiazole/

thiadiazide-phosphate esters and studied the anti-cancer characteristics on 10 cancer cell lines⁷. Although triazole derivatives can inhibit the proliferation of several cell types, their anti-cancer mechanism of action remains unclear.

In our continuing efforts to develop novel anti-lung cancer candidate compounds, we became interested in 3-aminotriazole. The common use of the 3-aminotriazole skeleton in many synthetic drugs indicates its potential as a new pharmacophore. In this study, we examined the anti-cancer properties of amino triazole derivatives to achieve better activity by appropriate structure modification (Figure 1). Amino triazole was present in the core of the designed compounds, with substituted phenyl groups introduced at positions 4 and 5. We hypothesised that a reasonable lipid–water partition coefficient could be obtained via

CONTACT Xian-yu Sun  sxianyu@163.com  Department of Pharmacy, College of Animal Science and Technique, Heilongjiang Bayi Agricultural University, Xinyang Road 2, 163319 Daqing, China; Cheng-hao Jin  jinchenghao3727@qq.com  Department of Biochemistry and Molecular Biology, College of Life Science and Technology, Heilongjiang Bayi Agricultural University, Xinyang Road 2, 163319 Daqing, China

 Supplemental data for this article is available online at [here](https://doi.org/10.1080/14756366.2019.1636044).

© 2019 The Author(s). Published by Informa UK Limited, trading as Taylor & Francis Group.

This is an Open Access article distributed under the terms of the Creative Commons Attribution License (<http://creativecommons.org/licenses/by/4.0/>), which permits unrestricted use, distribution, and reproduction in any medium, provided the original work is properly cited.

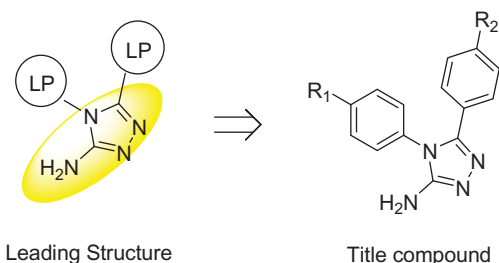


Figure 1. Design of the title compound. LP: Lipophilic group; the core is highlighted in yellow.

introduction of aromatic groups into the pharmacophore, thus enabling the target compound to easily penetrate the plasma membrane and enter the cell. Meanwhile, introduction of heterocyclic groups into amino triazole has been reported to increase its *in vitro* activity¹⁵. Thus, 4,5-(4-substituted)diphenyl-4H-1,2,4-triazol-3-amine derivatives were designed and prepared as potential anti-lung cancer agents. The incidence of lung cancer is related to various factors, and the mechanism of its induction is complex and diverse, whereas inhibition of lung cancer formation and metastasis is mainly regulated by induction of apoptosis. Expression of some apoptotic proteins is altered during apoptosis^{16,17}. In this study, the anti-cancer mechanisms of action of different compounds were evaluated from the perspective of apoptosis. The anti-cancer activities of these compounds were evaluated *in vitro*, and their structure–activity relations and anti-cancer mechanisms of action were investigated too.

2. Material and methods

2.1. Chemistry

Chromatography was conducted on silica gel 60, 200 mesh (Qingdao Haiyang, China), under high pressure supplied by an aquarium air pump (SB-2800). Analytical thin-layer chromatography (TLC) was performed on precoated silica gel 60 F254 plates (Qingdao Haiyang, China). The plates were visualised using UV light and/or iodine. Melting points (m.p.) were determined in open capillary tubes and were uncorrected. Chemical shifts are reported in ppm relative to tetramethyl silane. The structures of all the synthesised compounds were confirmed by ¹H, ¹³C nuclear magnetic resonance (NMR) spectroscopy and mass spectra. Mass spectra were recorded on an HP1100 LC/MSD electrospray ionisation mass spectrometer (Agilent Technologies, Santa Clara, CA, USA) and NMR spectra on an AV-300 FT-NMR spectrometer (Bruker BioSpin AG, Billerica, MA, USA). All the chemicals were of analytical grade. The detailed preparation process of compounds **4a–4j** is described below.

2.2. 4-Substituted-N-(4-chlorophenyl)benzamide (1a–1e) and 4-Substituted-N-phenylbenzamide (1f–1j)

A mixture of aromatic acid (10 mmol), aromatic amine (10 mmol), DMAP (10 mmol), and EDCI (10 mmol) in *N,N*-dimethyl formamide (DMF; 40 ml) was heated to 60 °C while stirring for 1 h. TLC revealed the completion of the reaction. After cooled, the mixture was filtered and washed with water, producing a light-white solid in 76.0–89.9% yield.

2.3. 4-Substituted-N-(4-chlorophenyl)benzothioamide (2a–2e) and 4-Substituted-N-phenylbenzothioamide (2f–2j)

A mixture of **1** (5 mmol), and Lawson reagent (5 mmol) in toluene (20 ml) was heated to reflux. After 24 h, the end of the reaction was confirmed by TLC. After cooling, the reaction mixture was filtered and evaporated to give a light-yellow solid as a crude product. The compounds obtained were pure enough for the following step.

2.4. N-Substituted phenyl-N'-amino substituted benzamide (3a–3j)

A mixture of **2** (5 mmol) and hydrazine hydrate (5 mmol) in ethanol (30 ml) was heated to 80 °C. After 1.5 h, the end of the reaction was confirmed by TLC. The reaction mixture was poured into cooled water (30 ml), and the precipitates was filtered and evaporated to give a light-white solid in 58.2–77.6% yield.

2.5. General synthetic procedure for target compounds (4a–4j)

In the presence of NaHCO₃, a mixture of compound **3** (1.0 mmol) and BrCN (1.1 mmol) in water (30 ml) was stirred at –5 °C 12–16 h. TLC showed that most of the starting material was reacted. The reaction mixture was extracted with dichloromethane (2 × 50 ml). The combined organic layers were dried over anhydrous MgSO₄, filtered, and evaporated; the residue was purified by silica gel column chromatography with ethyl acetate and methanol (8:1). The yields, m.p., and spectral data for each compound are shown below.

2.5.1. 4-(4-Chlorophenyl)-5-phenyl-4H-1,2,4-triazol-3-amine (4a)

Yield 80%, m.p. 168–170 °C; ¹H-NMR (300 MHz, CDCl₃), δ: 2.05 (s, 2H, –NH₂), 7.22–7.52 (m, 9H, Ar-H), ¹³C-NMR (300 MHz, CDCl₃), δ: 126.43, 127.83, 128.60, 128.63, 129.65, 130.83, 131.93, 136.22. ESI-MS m/z 271 (M + 1), 273 (M + 3), 274 (M + 4), calculated for [C₁₄H₁₁ClN₄] 270.

2.5.2. 4-(4-Chlorophenyl)-5-(4-bromophenyl)-4H-1,2,4-triazol-3-amine (4b)

Yield 79%, m.p. 248–250 °C; ¹H-NMR (300 MHz, CDCl₃), δ: 4.59 (s, 2H, –NH₂), 7.21–7.53 (m, 8H, Ar-H), ¹³C-NMR (300 MHz, CDCl₃), δ: 128.57, 129.09, 130.91, 131.85, 136.34. ESI-MS m/z 350 (M + 1), 351 (M + 2), calculated for [C₁₄H₁₀BrClN₄] 349.

2.5.3. 4,5-Bis(4-chlorophenyl)-4H-1,2,4-triazol-3-amine (4c)

Yield 86%, m.p. 247–248 °C; ¹H-NMR (300 MHz, CDCl₃), δ: 4.76 (s, 2H, –NH₂), 7.21–7.53 (m, 8H, Ar-H), ¹³C-NMR (300 MHz, CDCl₃), δ: 125.38, 128.58, 128.85, 128.88, 130.86, 132.14, 135.53, 136.20, 148.95, 154.80. ESI-MS m/z 307 (M + 2), 308 (M + 3), calculated for [C₁₄H₁₀Cl₂N₄] 305.

2.5.4. 4-(4-Chlorophenyl)-5-(4-fluorophenyl)-4H-1,2,4-triazol-3-amine (4d)

Yield 88%, m.p. 208–212 °C; ¹H-NMR (300 MHz, CDCl₃), δ: 4.31 (s, 2H, –NH₂), 6.95–7.52 (m, 8H, Ar-H), ¹³C-NMR (300 MHz, CDCl₃), δ: 115.66, 115.96, 122.81, 128.67, 129.74, 129.85, 130.83, 131.89, 136.26, 161.67, 164.99. ESI-MS m/z 289 (M + 1), 291 (M + 3), 292 (M + 4), calculated for [C₁₄H₁₀FCIN₄] 288.

2.5.5. 4-(4-Chlorophenyl)-5-(4-(methylsulfonyl)phenyl)-4H-1,2,4-triazol-3-amine (4e)

Yield 83%, m.p. >280 °C; ¹H-NMR (300 MHz, CDCl₃), δ: 3.05 (s, 3H, -CH₃), 4.63 (s, 2H, -NH₂), 7.24–7.88 (m, 8H, Ar-H), ¹³C-NMR (300 MHz, CDCl₃), δ: 43.65, 127.63, 127.96, 130.31, 130.69, 132.66, 132.98, 134.64, 140.90, 147.54, 156.82. ESI-MS m/z 349 (M + 1), 351 (M + 3), calculated for [C₁₅H₁₃O₂N₄] 348.

2.5.6. 4-Phenyl-5-(4-bromophenyl)-4H-1,2,4-triazol-3-amine (4f)

Yield 86%, m.p. 268–271 °C; ¹H-NMR (300 MHz, CDCl₃), δ: 4.58 (s, 2H, -NH₂), 7.22–7.56 (m, 8H, Ar-H), ¹³C-NMR (300 MHz, CDCl₃), δ: 123.64, 126.04, 127.25, 129.02, 130.63, 131.69, 133.63. ESI-MS m/z 317 (M + 1), 318 (M + 2), calculated for [C₁₄H₁₁BrN₄] 316.

2.5.7. 4-Phenyl-5-(4-chlorophenyl)-4H-1,2,4-triazol-3-amine (4g)

Yield 83%, m.p. 243–246 °C; ¹H-NMR (300 MHz, CDCl₃), δ: 4.65 (s, 2H, -NH₂), 7.20–7.55 (m, 9H, Ar-H), ¹³C-NMR (300 MHz, CDCl₃), δ: 125.41, 127.28, 128.77, 128.86, 130.18, 130.66, 133.44, 135.46. ESI-MS m/z 271 (M + 1), 273 (M + 3), calculated for [C₁₄H₁₁ClN₄] 270.

2.5.8. 4-Phenyl-5-(4-fluorophenyl)-4H-1,2,4-triazol-3-amine (4h)

Yield 81%, m.p. 207–211 °C; ¹H-NMR (300 MHz, CDCl₃), δ: 4.64 (s, 2H, -NH₂), 6.91–7.55 (m, 9H, Ar-H), ¹³C-NMR (300 MHz, CDCl₃), δ: 115.42, 115.71, 123.46, 127.30, 128.81, 129.57, 129.68, 129.95, 130.52, 130.85, 133.78, 149.15, 154.77, 161.48, 164.79. ESI-MS m/z 255 (M + 1), calculated for [C₁₄H₁₁FN₄] 254.

2.5.9. 4-Phenyl-5-(4-methylphenyl)-4H-1,2,4-triazol-3-amine (4i)

Yield 76%, m.p. 245–250 °C; ¹H-NMR (300 MHz, CDCl₃), δ: 1.23–1.28 (t, J = 6 Hz, 9H, -CH₃), 4.54 (s, 2H, -NH₂), 7.04–7.53 (m, 8H, Ar-H), ¹³C-NMR (300 MHz, CDCl₃), δ: 21.24, 124.31, 127.35, 127.59, 129.08, 129.74, 130.38, 134.04, 139.25. ESI-MS m/z 251 (M + 1), calculated for [C₁₅H₁₄N₄] 250.

2.5.10. 4-Phenyl-5-(4-(trifluoromethyl)phenyl)-4H-1,2,4-triazol-3-amine (4j)

Yield 86%, m.p. 222–225 °C; ¹H-NMR (300 MHz, CDCl₃), δ: 4.90 (s, 2H, -NH₂), 7.27–7.58 (m, 9H, Ar-H), ¹³C-NMR (300 MHz, CDCl₃), δ: 125.40, 125.45, 127.24, 127.61, 130.30, 130.50, 130.77, 133.51, 148.64, 155.71. ESI-MS m/z 305 (M + 1), 306 (M + 2), calculated for [C₁₄H₁₁CF₃N₄] 304.

2.6. The cell viability assay

The three lung cancer cell lines, A549, NCI-H460, and NCI-H23, and three normal cell lines, normal lung IMR-90 cells, normal liver L-02 cells, and normal gastric GES-1 cells, were acquired from the American Type Culture Collection (Manassas, VA, USA). The cells were cultured in RPMI-1640 supplemented with 10% of foetal bovine serum, 100 U/mL penicillin, and 100 µg/mL streptomycin (Gibco, Grand Island, NY, USA), at 5% CO₂ and 37 °C. The cells were monitored daily and maintained at 80% cell density¹⁸.

Cell viability was determined by the MTT assay. Lung cancer cells (A549, NCI-H460, and NCI-H23) and normal human lung IMR-90 cells, liver L-02, and gastric GES-1 cells were harvested during the logarithmic phase of growth. All the cells were seeded in 96-well plates at 10⁴ cells/well and then treated with

various concentrations (0.1, 0.3, 1.0, 3.0, or 30 µmol/mL) of 5-FU or one of amino triazole derivatives for 24 h. The MTT solution (15 µL; 5 mg/mL) was added into each well, and the cells were cultured for 4 h at 37 °C. The supernatants were removed, and resolved with 100 µL of DMSO, and the cells were shocked for 10 min. The optical density of the samples was measured at 490 nm on a microplate luminometer. Cell viability was expressed as the percentage change in absorbance compared to the control values.

2.7. Cell apoptosis analysis

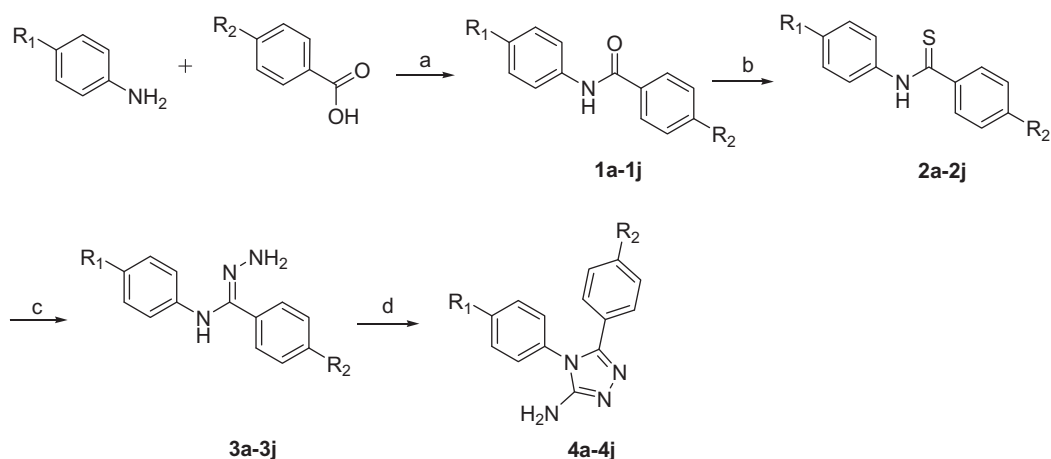
Apoptosis and necrosis were analysed by Hoechst/ propidium iodide (PI) double staining and early and late apoptosis were analysed by Annexin V/PI flow cytometry. A549 cells were seeded in 6-well plates (10⁵ cells/well) and treated with 2 µM 5-FU or one of amino triazole derivatives for 0, 3, 6, 12, and 24 h. After that, the cells were collected and washed once in phosphate-buffered saline (PBS). The cells were resuspended in 195 µL of binding buffer, and dual staining was performed with 3 µL of Hoechst or Annexin V and 2 µL of PI, and the cells were incubated for 20 min at room temperature in the dark. Apoptotic cells were analysed using the EVOS FL Auto Cell Imaging System (Thermo Fisher Scientific, Inc., Waltham, MA, USA) and a flow cytometer (Beckman Coulter, Inc., Brea, CA).

2.8. Western blotting analysis

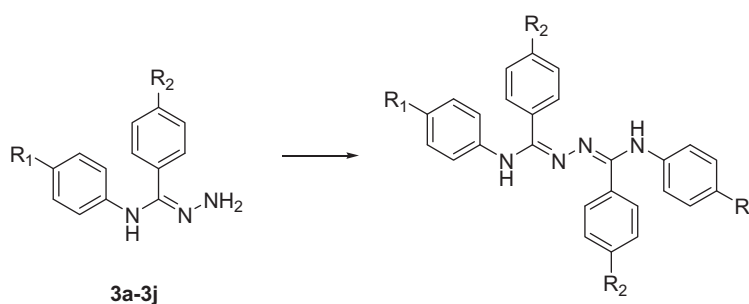
A549 cells were washed with PBS and lysed in cell extraction buffer (1 M 4-[2-hydroxyethyl]-1-piperazineethanesulfonic acid [HEPES] pH 7.0, 5 M NaCl, 0.5% Triton X-100, 10% of glycerol, 20 mM β-mercaptothion, 20 mg/mL 4-(2-aminoethyl)benzenesulfonyl fluoride hydrochloride [AEBSF], 0.5 mg/mL pepstatin, 0.5 mg/mL leupeptin, and 2 mg/mL aprotinin). Cell lysates were centrifuged for 30 min at 12,000 × g and 4 °C. Aliquots of the lysates were separated by sodium dodecyl sulphate polyacrylamide gel electrophoresis in a 10% gel and transferred onto nitrocellulose membranes. The membranes were blocked for 1 h with 5% skim milk at room temperature, incubated for 12 h with primary antibodies: mouse monoclonal antibodies against α-tubulin, BAX, BCL-2, cleaved poly[ADP-ribose] polymerase (cle-PARP), and then cleaved caspase 3 at 4 °C (all from Santa Cruz Biotechnology, Inc., Dallas, TX). The membranes were washed with Tris-buffered saline supplemented with 0.1% Tween 20 (TBST) and incubated with secondary antibodies: a goat anti-rabbit IgG antibody or goat anti-mouse IgG antibody at room temperature for 2 h. The Pierce ECL reagent (Rockford, IL, USA) was added, and the bands were detected on an Amersham Imager 600 (GE, Little Chalfont, UK) and quantified in the ImageJ software (NIH, Bethesda, MD, USA). Relative protein expression in the treated cells was compared to that in the control group. The endogenous control was α-tubulin.

2.9. Statistical analysis

This procedure was performed by one-way analysis of variance in SPSS 19.0 software (SPSS, Inc., Chicago, IL, USA), and the results are presented as the means ± SD. A value of *p* < .05 was assumed to indicate statistical significance.

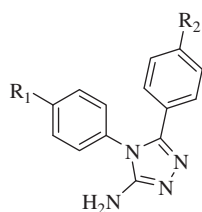


Scheme 1. Synthesis of target compounds **4a-4j**. (a) EDCI, DMAP, DMF, 60 °C; (b) Lawesson's reagent, methylbenzene, 100 °C; (c) N₂H₄ H₂O, EtOH, 80 °C; (d): NaHCO₃, BrCN, -5 °C.



Scheme 2. Structural change in compounds **3a-3j**.

Table 1. IC₅₀ (μM) values of 5-FU and of amino triazole derivatives towards lung cancer cells.



Comp.	R ₁	R ₂	Lung cancer cells			cLogP
			A549	NCI-H460	NCI-H23	
5-FU	-	-	28.24 ± 1.53	61.56 ± 3.62	33.68 ± 1.34	-
4a	Cl	H	1.23 ± 0.08	8.52 ± 0.41	6.94 ± 0.36	4.10
4b	Cl	Br	1.02 ± 0.05	7.27 ± 0.42	6.06 ± 0.44	5.14
4c (BCTA)	Cl	Cl	1.09 ± 0.06	2.01 ± 0.11	3.28 ± 0.15	4.87
4d	Cl	F	2.32 ± 0.18	7.59 ± 0.43	7.91 ± 0.48	4.32
4e	Cl	SO ₂ CH ₃	45.02 ± 2.83	>100	45.43 ± 2.79	2.84
4f	H	Br	48.01 ± 3.86	32.04 ± 1.85	42.66 ± 3.78	4.45
4g	H	Cl	3.16 ± 0.45	8.77 ± 0.55	9.04 ± 0.74	4.27
4h	H	F	3.64 ± 0.32	10.98 ± 1.02	9.61 ± 0.81	3.74
4i	H	CH ₃	11.32 ± 1.37	15.69 ± 1.56	18.04 ± 1.64	3.97
4j	H	CF ₃	31.22 ± 2.54	70.36 ± 4.69	37.81 ± 2.63	4.48

IC₅₀: Each value was averaged by three parallel groups of eight repeats and calculated using a SigmaPlot software. cLogP: It was obtained by analysing the chemical properties of structures in Chemdraw software.

3. Results and discussion

3.1. Chemistry

A series of 4,5-(substituted phenyl)-4H-1,2,4-triazol-3-amine derivatives (**4a-4j**) was designed and synthesised according to

Scheme 1. Compounds **1a-1j** were prepared by reacting *p*-substituted aniline and *p*-substituted benzoic acid with EDCI and DMAP in dimethylformamide (DMF)¹⁹. The oxygen atoms of compounds **1a-1j** were converted to sulphur atoms by Lawesson's reagent in refluxing toluene to produce compounds **2a-2j**²⁰. Compounds **3a-3j** were obtained in a 70–80% yield by means of hydrazine hydrate at 80 °C. Compounds **4a-4j** were prepared by reacting compounds **3a-3j** with cyanogen bromide (BrCN) and sodium bicarbonate in water at -5 °C. If the reaction temperature was >0 °C, a structural change was detected, as shown in **Scheme 2**, and the molecular weight indicated that di-substitution had occurred. Nonetheless, this change was avoided by maintaining the reaction mixture at -5 °C.

3.2. The viability of lung cancer cells treated with 4a-4j

The synthesised compounds were subjected to the cytotoxicity assay by the 3-(4,5-dimethylthiazol-2-yl)-2,5-diphenyltetrazolium bromide (MTT) method as described previously²¹. IC₅₀ is defined as the drug concentration causing a 50% reduction of cell number compared with that of untreated control. In the first screening, we evaluated the effects of the compounds on the growth of three lung cancer cell lines (A549, NCI-H460, and NCI-H23). Their anti-cancer activities were measured and are presented in **Table 1**. The results were averages of three separate measurements. 5-Fluorouracil (5-FU) served as a positive control.

As presented in **Table 1**, most compounds significantly inhibited the growth of three lung cancer cell lines in a dose-dependent manner. Seven compounds were found to be more potent than 5-FU. The most potent compound **4c**

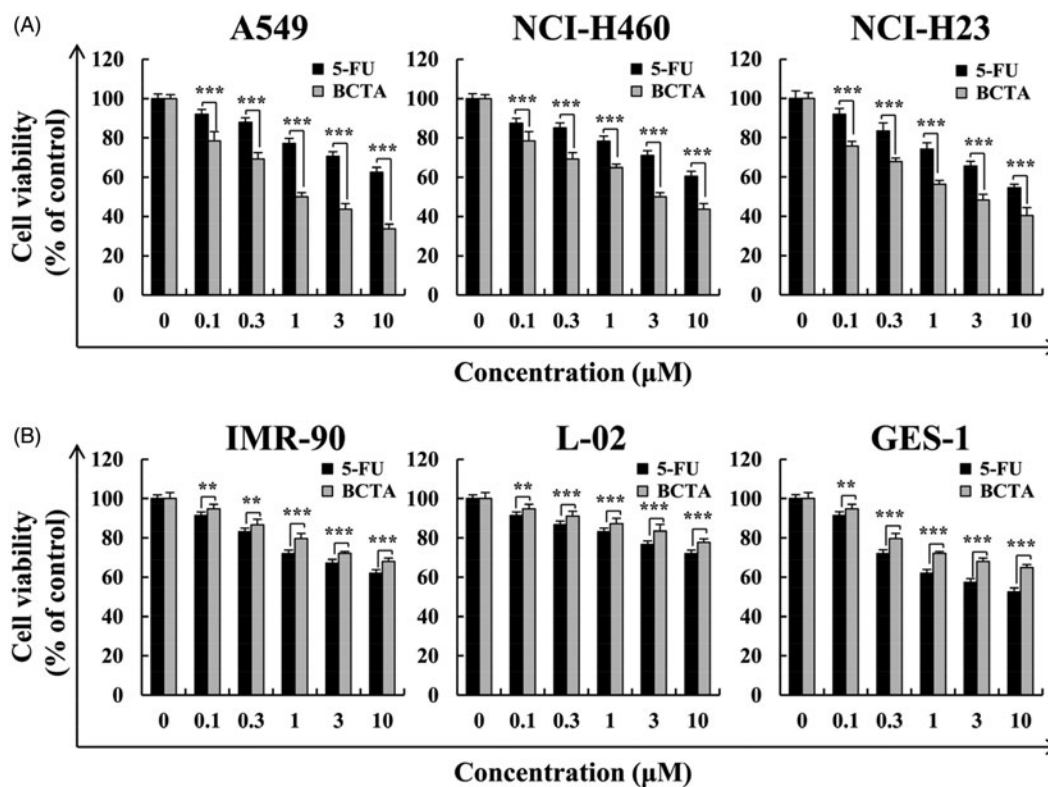


Figure 2. Effects of BCTA on cell viability in human lung cancer cells. (A) Three human lung cancer cell lines (A549, NCI-H460, and NCI-H23) and (B) three normal cell lines (IMR-90, L-02, and GES-1) were treated with different concentrations (0.1, 0.3, 1.0, 3.0, or 30 μM) of 5-FU or BCTA for 24 h. Error bars indicate the means \pm SD of three independent experiments (* $p < .05$, ** $p < .01$, *** $p < .001$ indicate significant differences).

(4,5-bis(4-chlorophenyl)-4H-1,2,4-triazol-3-amine, **BCTA**) exerted cytotoxicity 10- to 20-fold more potent than that of 5-FU with IC_{50} of 1.09 μM towards A549 cells, 2.01 μM towards NCI-H460 cells, and 3.28 μM towards NCI-H23 cells, respectively, at 24 h.

Furthermore, the cytotoxic effects of **BCTA** were significantly weaker (as compared to treatment with 5-FU) towards normal lung IMR-90, liver L-02, and gastric GES-1 cells (Figure 2). A549 cells showed the highest sensitivity to these compounds, and thus we choose these cells for further analysis.

3.3. BCTA-induced apoptosis in A549 cells

To determine whether amino triazole derivatives induce A549 cell apoptosis, we conducted Hoechst/PI double staining and an annexin V/PI flow-cytometric assay to elucidate the mechanism. As depicted in Figure 3(A,B), the experimental group was significantly better than the control treatment 5-FU. Particularly, at 12 and 24 h, **BCTA** treatment resulted in a 64% apoptosis rate, which was higher than the rate caused by 5-FU: 35%. According to the results of flow cytometry, the apoptosis rate afforded by **BCTA** was 55.5% (Figure 3(C,D)), and the results were nearly consistent with those of Hoechst/PI staining.

3.4. Western blotting result of BCTA in A549 cells

For further evaluation of intrinsic apoptosis mechanism, **BCTA** was tested for its effect on the expression of four critical peptides. Results of the Western blotting analysis were expressed as the relative tation of the specific band compared with the internal reference. **BCTA** clearly increased the protein expression levels of BAX,

caspase 3, and PARP and decreased the protein expression levels of BCL-2 (Figure 4(A,B)) in a time dependence manner (3–24 h). The results suggested that **BCTA** induced apoptosis in A549 cells by up-regulating the mitochondrial apoptotic pathways.

3.4. Discussion

Amino triazole derivatives have been reported to possess a broad range of biological and pharmacological properties, such as anti-bacterial, anti-human immunodeficiency virus, anti-microbial, anti-fungal, anti-viral, and anti-cancer effects. Nevertheless, their anti-cancer mechanism of action remains unclear. Because this is our first study on the compounds carrying the 3-aminotriazole moiety as potential anti-cancer agents, we initially designed 10 compounds to roughly identify general structural features required for anti-cancer cytotoxicity. This study uncovered a part of the mechanism of action, and the relation between its structure and anti-cancer activity through pharmacological analysis. The results showed that the compounds induced apoptosis in tumour cells and inhibited cell proliferation by changing the expression of relevant proteins to achieve anti-cancer activity. The strength of this anti-cancer activity was found to be related to various substituents. According to Table 1, the anti-neoplastic activities of four chlorobenzene-substituted compounds (**4a–4d**) were significantly better than those of the 5-phenyl-4H-1,2,4-triazol-3-amine structures (**4f–4j**). Our results showed that their toxicity (particularly that of **BCTA**) towards normal cells was less than that of 5-FU in the control group.

It is well known that the activity of drugs is mainly determined by their structure. One of the main factors is the lipid–water distribution coefficient (LogP value). LogP is an interpretation of the

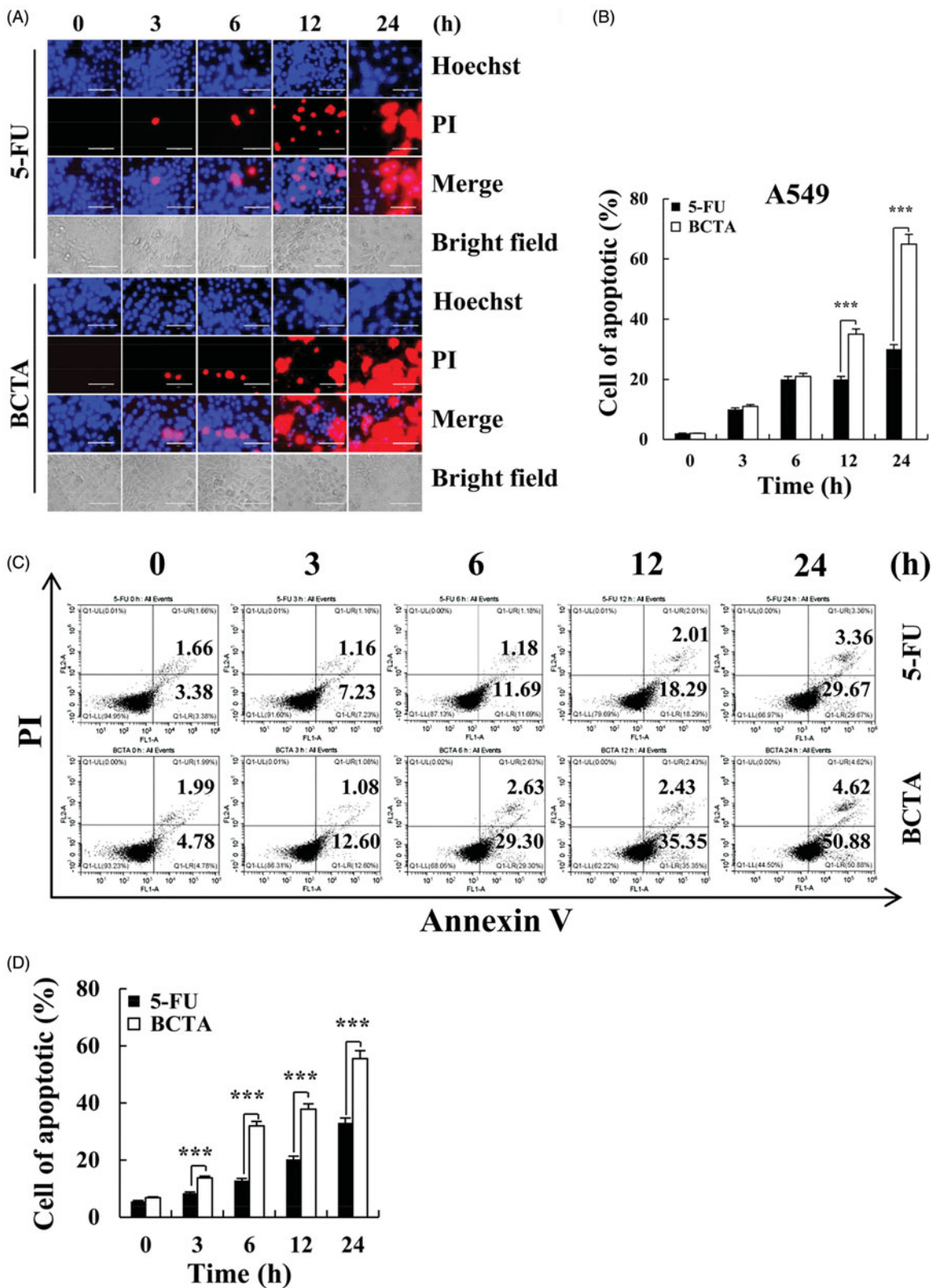


Figure 3. Induction of apoptosis and necrosis by BCTA in A549 cells. (A) A549 cells were treated with 2 μ mol/mL of BCTA or 5-FU for different periods (0, 3, 6, 12, or 24 h) and stained with the Hoechst/PI solution. The morphology and fluorescence intensity were examined under a fluorescence microscope (magnification: $\times 200$). (B) Quantification of fluorescence intensity. (C) A549 cells were treated with 2 μ mol/mL BCTA or 5-FU for 0, 3, 6, 12, or 24 h, stained with the annexin V/PI solution, and analysed by flow cytometry. (D) Quantification of the percentages of apoptotic cells. Error bars indicate the means \pm SD of three independent experiments (* $p < .05$, ** $p < .01$, *** $p < .001$ indicate significant differences).

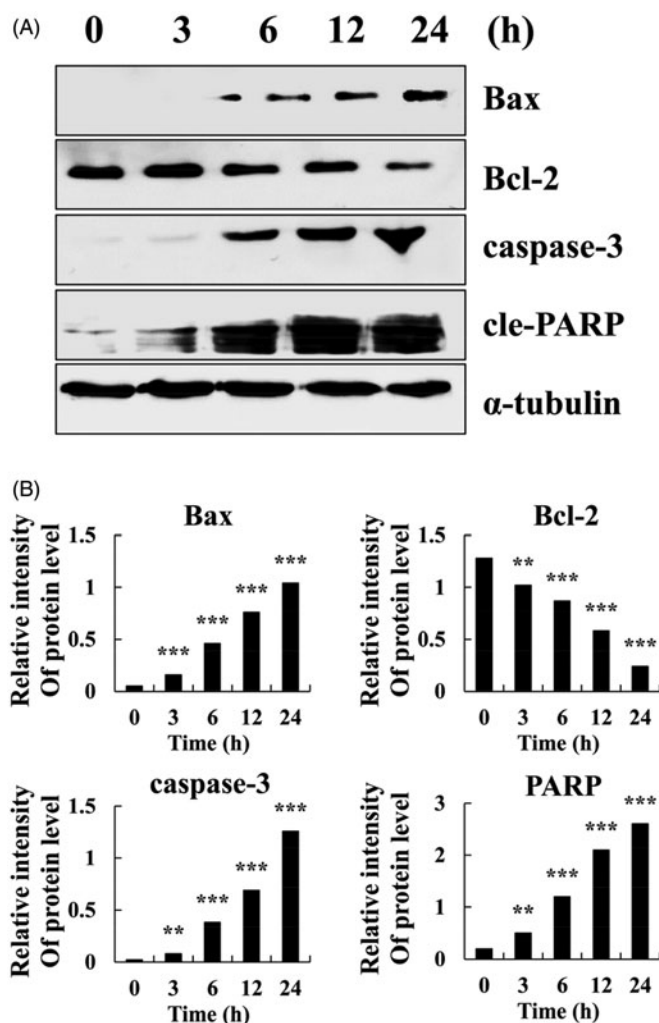


Figure 4. Apoptotic effects of BCTA on A549 cells. (A) Effects of BCTA on the expression levels of BAX, BCL-2, caspase 3, and cleaved PARP in A549 lung cancer cells were analysed by western blotting and (B) densitometric quantification. * $p < .05$, ** $p < .01$, *** $p < .001$ relative to the control group (0 h). BCL-2, B-cell lymphoma 2; BAX, BCL-2-associated agonist of cell death; cle-PARP, cleaved poly (adenosine diphosphate ribose) polymerase.

lipid phase and water phase equilibrium ratio of compounds. It can also be employed to determine pharmacological parameters. An increase in the lipid–water distribution coefficient indicates increased solubility of the compound in fat; in contrast, a decrease in this coefficient means increased solubility in water. The solubility of a compound in fatty substances present in the body is known as the hydrophobicity of that compound, whereas the solubility of a compound in water is known as hydrophilicity of that compound. The human body absorbs hydrophilic compounds more easily because of its high water content²². Nonetheless, the cell membrane has a phospholipid bilayer structure that is lipophilic in nature. Thus, if a hydrophilic component of a compound is too large, it cannot enter the cell. Therefore, anti-cancer compounds should be lipophilic to some extent. The extent of drug absorption may also be affected by the magnitude of the LogP value. Hence, an optimal LogP value is necessary to allow a material to easily enter the cell membrane and participate in biological functions. The optimal value for cLogP is approximately 5²³. Due to the complexity of factors affecting drug activity, a drug needs a suitable cLogP value, but an appropriate cLogP value does not guarantee a good activity. As shown in Table 1, compound **4b** and **BCTA** seem to be two promising structures.

In-depth analysis of the structure–activity relationship of these structures revealed that most of the tested compounds exerted a cytotoxic activity against lung cancer cells (IC_{50} 1.02–48.01 μ M). The compounds containing a halogen atom on the phenyl ring showed better activity than did the compounds without a halogen atom. We also found that the Cl atom contributed more to the toxicity towards lung cancer cells than Br and F atoms did. As shown in Table 1, **BCTA** showed the strongest activity against lung cancer cell lines A549, NCI-H460, and NCI-H23 with IC_{50} values of 1.09–3.28 μ M. Similarly, **4g** (4-phenyl, 5-(*p*-Cl)phenyl) exerted a stronger activity against lung cancer cells than did **4f** (4-phenyl, 5-(*p*-Br)phenyl) and **4h** (4-phenyl, 5-(*p*-F)phenyl). Meanwhile, compounds **4a** (5-phenyl), **4b** (5-(*p*-Br)phenyl), and **4d** (5-(*p*-F)phenyl) also possess good activity against three lung cancer cells. This level of growth inhibition was multiple stronger than that of 5-FU against lung cancer cells. IC_{50} values of derivatives **4e** (4-(4-chlorophenyl), 5-(*p*-SO₂CH₃)phenyl) and **4h** (4-phenyl, 5-(*p*-CH₃)phenyl) against lung cancer cells were higher (worse) than IC_{50} of the control group (5-FU). Thus, no significant difference was observed in the activity between the compounds containing electron-donating groups and those containing electron-withdrawing groups.

As discussed above, most of the synthesised compounds with a halogen atom at the *para*-position of the 5-phenyl ring manifested a strong toxic activity against lung cancer cells. Finally, compound **BCTA** was the most potent cytotoxic agent, with IC_{50} values of 1.09, 2.01, and 3.28 μ M against A549, NCI-H460, and NCI-H23 cells, respectively. These IC_{50} values were many times stronger than those of the reference agent 5-FU. So, compound **BCTA** was further screened its apoptosis-inducing capability and possible action mechanism.

Apoptosis is a conserved programmed cell death mechanism involved in the elimination of cancer cells^{24,25}. Intrinsic apoptosis depends on factors released from the mitochondria and is also known as mitochondrial apoptosis²⁶. The mitochondrial pathway is regulated by BCL-2 family members, which include pro-apoptotic protein BAX and anti-apoptotic protein BCL-2. Caspase 3 is a critical enzyme in apoptosis because it cleaves several essential cellular proteins such as PARP²⁷. Many anti-cancer agents induce the intrinsic apoptotic pathway, which is characterised by activation of caspase 3 and cleavage of PARP²⁸. The present study indicates that amino triazole derivatives significantly induced the apoptosis of A549 cells by up-regulating BAX, down-regulating BCL-2, and activating caspase 3 and PARP. These findings suggest that amino triazole derivatives regulate BCL-2 and BAX expression and activate the mitochondrial apoptotic cascade in lung cancer cells.

4. Conclusions

In summary, we synthesised novel amino triazole derivatives, particularly 4,5-bis (4-chlorophenyl)-4*H*-1,2,4-triazol-3-amine (**BCTA**), and investigated the anti-cancer molecular mechanisms of action of **BCTA**. **BCTA** induced apoptosis in human lung cancer cells by triggering the apoptosis pathways. On the basis of our observations, **BCTA** is a promising candidate for the development of anti-lung cancer drugs.

Disclosure statement

No potential conflict of interest was reported by the authors.

Funding

The authors are grateful for the financial support from the National Natural Science Foundation of China [Grant No. 81502922], and Programme for Young Scholars with Creative Talents in HeiLongJiang BaYi Agricultural University [CXRC2016-9]. Authors also thank the funding support of Heilongjiang Bayi Agricultural University graduate students innovation project [2011150102].

ORCID

Cheng-hao Jin  <http://orcid.org/0000-0003-4431-2623>

References

- Bray F, Ferlay J, Soerjomataram I, et al. Global cancer statistics 2018: GLOBOCAN estimates of incidence and mortality worldwide for 36 cancers in 185 countries. *CA Cancer J Clin* 2018;68:394–424.
- Wang Q, Ma C, Li X, et al. Synthesis of novel sugar or azasugar modified anthra[1,2-d]imidazole-6,11-dione derivatives and biological evaluation. *Carbohydrate Res* 2018;460:29–33.
- Gazieva GA, Anikina LV, Nechaeva TV, et al. Synthesis and biological evaluation of new substituted thioglycolurils, their analogues and derivatives. *Eur J Med Chem* 2017;140:141–54.
- Osmaniye D, Kaya Cavusoglu B, Saglik B, et al. Synthesis and anticandidal activity of new imidazole-chalcones. *Molecules* 2018;23:831.
- Liu Y, Peng Y, Lu J, et al. Design, synthesis, and biological evaluation of new 1,2,3-triazolo-2'-deoxy-2'-fluoro-4'-azido nucleoside derivatives as potent anti-HBV agents. *Eur J Med Chem* 2018;143:137–49.
- Hafez HN, Alsalamah SA, El-Gazzar AR. Synthesis of thiophene and N-substituted thieno [3,2-d] pyrimidine derivatives as potent antitumor and antibacterial agents. *Acta Pharm* 2017;67:275–92.
- Abdou WM, Ganoub NA, Sabry E. Design, synthesis and pharmacological screening of β -amino-, thiadiazole/thiadiazine-phosphonate based triazole motifs as antimicrobial/cytotoxic agents. *Acta Pharm* 2014;64:267–84.
- Liu Y, Xia Y, Fan Y, et al. N-Aryl triazole ribonucleosides with potent antiproliferative activity against drug-resistant pancreatic cancer. *Bioorganic Med Chem Letters* 2010;20:2503–7.
- Çikla-Süzgün P, Kaushik-Basu N, Basu A, et al. Anti-cancer and anti-hepatitis C virus NS5B polymerase activity of etodolac 1,2,4-triazoles. *J Enzyme Inhib Med Chem* 2015;30:778–85.
- Mustafa M, Abdelhamid D, Abdelhafez EMN, et al. Synthesis, antiproliferative, anti-tubulin activity, and docking study of new 1,2,4-triazoles as potential combretastatin analogues. *Eur J Med Chem* 2017;141:293–305.
- Ohsumi K, Hatanaka T, Fujita K, et al. Syntheses and antitumor activity of cis-restricted combretastatins: 5-membered heterocyclic analogues. *Bioorg Med Chem Lett* 1998;8:3153–8.
- Driowya M, Leclercq J, Verones V, et al. Synthesis of triazoloquinazolinone based compounds as tubulin polymerization inhibitors and vascular disrupting agents. *Eur J Med Chem* 2016;115:393–405.
- Alanazi AM, Abdel-Aziz AAM, Shower TZ, et al. Synthesis, antitumor and antimicrobial activity of some new 6-methyl-3-phenyl-4(3H)-quinazolinone analogues: in silico studies. *J Enzyme Inhib Med Chem* 2016;31:721–35.
- Fodor M, Price E, Wang P, et al. Dual allosteric inhibition of SHP2 phosphatase. *ACS Chem Biol* 2018;13:647–56.
- Ferrini S, Chandanshive JZ, Lena S, et al. Ruthenium-catalyzed synthesis of 5-amino-1,2,3-triazole-4-carboxylates for triazole-based scaffolds: beyond the Dimroth rearrangement. *J Org Chem* 2015;80:2562–72.
- Shao B, Wei X, Luo M, et al. Inhibition of A20 expression in tumor microenvironment exerts anti-tumor effect through inducing myeloid-derived suppressor cells apoptosis. *Sci Rep* 2015;5:16437.
- Luan Z, He Y, He F, et al. Rocaglamide overcomes tumor necrosis factor-related apoptosis-inducing ligand resistance in hepatocellular carcinoma cells by attenuating the inhibition of caspase-8 through cellular FLICE-like-inhibitory protein down regulation. *Mol Med Rep* 2015;11:203–11.
- Hany AME, Bahaa GMY, Syed NAB, et al. Synthesis, anti-cancer activity and molecular modeling studies of 1,2,4-triazole derivatives as EGFR inhibitors. *Eur J Med Chem* 2018;156:774–89.
- Dantale S, Reboul V, Metzner P, et al. First use of axially chiral thioamides for the stereocontrol of C-C bond formation. *Chem A Eur J* 2002;8:632–40.
- Yang CH, Li GJ, Gong CJ, et al. N, N-dialkylaniline-assisted thionation of carboxylic amides and esters. *Tetrahedron* 2015;71:637–42.
- Zhang HJ, Zhang GR, Piao HR, et al. Synthesis and characterisation of celastrol derivatives as potential anticancer agents. *J Enzyme Inhib Med Chem* 2018;33:190–8.
- Sun XY, Zhong CY, Liu MY, et al. Design, synthesis and activity evaluation of 2-ethyl-1-(4-substituted) phenyl-1H-imidazole derivatives as potent antibacterial agents. *Latin Am J Pharmacy* 2018;37:768–74.
- Nishida H, Arikawa Y, Hirase K, et al. Identification of a novel fluoropyrrole derivative as a potassium-competitive acid blocker with long duration of action. *Bioorg Med Chem* 2017;25:3298–314.
- Meng LQ, Liu C, Luo YH, et al. Quinalizarin exerts an anti-tumour effect on lung cancer A549 cells by modulating the Akt, MAPK, STAT3 and p53 signalling pathways. *Mol Med Rep* 2018;17:2626–34.
- Wang JR, Shen GN, Luo YH, et al. The compound 2-(naphthalene-2-thio)-5, 8-dimethoxy-1,4-naphthoquinone induces apoptosis via reactive oxygen species-regulated mitogen-activated protein kinase, protein kinase B, and signal transducer and activator of transcription 3 signaling in human gastric cancer cells. *Drug Dev Res* 2018;79:295–306.
- Wang F, Wei ZL, Sun XR, et al. Apoptosis inducing factor is involved in stretch-induced apoptosis of myoblast via a caspase-9 independent pathway. *J Cell Biochem* 2017;118:829–38.
- Hassan M, Watari H, AbuAlmaaty A, et al. Sakuragi, apoptosis and molecular targeting therapy in cancer. *BioMed Res Int* 2014;2014:1–23.
- Melissa DA, Gunning PW, Stehn JR. Tumor suppressor tropomyosin Tpm2. 1 regulates sensitivity to apoptosis beyond anoikis characterized by changes in the levels of intrinsic apoptosis proteins. *Cytoskeleton* 2017;74:233–48.